Purdue University
Purdue e-Pubs

International Compressor Engineering Conference School of Mechanical Engineering

2016

3D Compressible Simulation Of a Muffler With Pseudosound Prediction Levels

Jesus Ruano
CTTC, Universitat Politecnica de Catalunya, Spain, jesusr@cttc.upc.edu

Joan Lopez
CTTC, Universitat Politecnica de Catalunya, Spain, joanl@cttc.upc.edu

Oriol Lehmkuhl
CTTC, Universitat Politecnica de Catalunya, Spain, oriol@cttc.upc.edu

Joaquim Rigola
CTTC, Universitat Politecnica de Catalunya, Spain, quim@cttc.upc.edu

Carles David Pérez Segarra
CTTC, Universitat Politecnica de Catalunya, Spain, segarra@cttc.upc.edu

3D Compressible Simulation Of a Muffler With Pseudosound Prediction Levels

Jesús RUANO[1*], Joan LÓPEZ[1], Oriol LEHMKUHL[1], Joaquim RIGOLA[1], Carles David PÉREZ SEGARRA[1]

[1]Heat and Mass Transfer Technological Center (CTTC)
Universitat Politècnica de Catalunya – Barcelona TECH (UPC),
Colom, 11, E-08222, Terrassa (Barcelona), Spain
Tel. +34 93 739 81 92
Email: cttc@cttc.upc.edu, http://www.cttc.upc.edu

* Corresponding Author

ABSTRACT

The main objective of this paper is to present a numerical resolution of a suction muffler configuration by using an in-house object oriented CFD & HT code TermoFluids (Lehmkuhl et al. 2007), able to handle tridimensional geometries, unstructured meshes with intrinsic parallelization. This code has been adapted to be able to resolute 3D Navier-Stokes equations in their compressible form and coupled with the numerical resolution of the whole compressor domain by means of a parallel and object-oriented called NEST (Lopez, 2016).

The numerical results aim to study the influence of the suction muffler inner geometry in the fluidynamic behavior inside the muffler while considering how this internal geometry affects the global performance of the compressor. Hence, the inlet and outlet boundary conditions at the muffler are obtained from the numerical simulation of the whole compressor using NEST, while the fluid behavior inside the muffler is numerically simulated by means of detailed analysis. The paper presents a methodology that handles with Large Eddy Simulation (LES) models for the turbulent motion of fluid inside the muffler, the formulation of Navier-Stokes in their compressible form, dealing with numerical problems derived from the compressible part, and the coupling of the whole compressor simulation to set boundary condition.

1. INTRODUCTION

The understanding of the physical phenomena happening inside a reciprocating compressor is a must to improve its design and efficiency. However, nowadays is still a challenging problem due the fluid inside the compressor is submitted to periodic changes mainly in its pressure and velocity and consequently to all the thermo-dynamical values associated with them. Hence, a numerical code used to simulate compressors must be able to handle with the compressible nature of the refrigerant and the periodicity of the variations in the main values of the fluid.

One-dimensional models are one of the most used tools to numerically analyze compressors. These models offer a faster simulation rather than conventional CFD & HT simulations, where the three dimensionality of the problem is taken into account. The great improvement in speed makes possible the comparison of different geometries and configurations in a relative short period (Rigola, 2002).

While one-dimensional models have been used to study mufflers since more than 40 years, three-dimensional simulations had recently begun to be adopted by the community. While several authors have relied on constant boundary conditions (Choi, 2002), Sarioglu (2012) simulated a full cycle inside the muffler using time dependent boundary conditions extracted from an empirical study. Done (2014) simulated different muffler geometries imposing acoustic pressure at inlet and measuring the outlet signal. His study also shown although fluid-dynamics can be correctly computed with one-dimensional models; acoustics at medium-high frequencies are wrongly computed if three-dimensional models are not taken into account.

The present paper is focused on the numerical resolution of a muffler using 3D unstructured, parallel and object oriented CFD & HT code TermoFluids (Lehmkuhl et al. 2007). This in-house code uses Large Eddy Simulation (LES) turbulence models instead of classical Reynolds Averaged Navier-Stokes equations (RANS). As a post process, the spectrum of the pressure at both inlet and outlet will be analyzed in order to understand muffler's behavior towards pseudonoise generation and propagation trough the component.

2. NUMERICAL METHOD

The numerical simulation of the suction muffler is based on a 3D explicit finite volume method adapted to compressible flows and integrated in time by using a second order Adams-Bashford time scheme. Turbulence modeling is an extension of Wall-Adapting Local Eddy-viscosity (WALE) (Nicoud, F. and Ducros., 1999) to unstructured meshes. These methods have been implemented in an in-house code TermoFluids (Lehmkuhl *et al.*, 2007).

2.1 Navier-Stokes equations

The main features of the discretized Navier-Stokes equations in its compressible form will be presented here. The compressible form of Navier-Stokes equations takes into account the effect of density variations, which are of high importance inside a compressor. If these variations want to be taken into account then momentum equations alone are not enough to simulate the problem; density and energy equations as well as a state equation are necessary to be added to the set of equations to correctly simulate the problem.

$$\Omega_c \frac{\partial \rho_c}{\partial t} + M u_c = 0 \tag{1}$$

$$\Omega_c \frac{\partial (\rho_c u_c)}{\partial t} + C(\rho_c u_c) u_c + D u_c + \Omega_c G p_c = 0 \tag{2}$$

$$\Omega_c \frac{\partial (\rho_c h_c)}{\partial t} + C(\rho_c u_c) h_c + D T_c + \tau : G u_c = 0 \tag{3}$$

The modeled substance is assumed to follow real gas law, being the selected equation the ideal gas law with compressibility factor calculated via acentric factor:

$$p = z \rho R T \tag{5}$$

$$z = z_0 + \omega \cdot z_1 \tag{6}$$

$$z_0 = 1 + (0.083 - 0.422/T_r^{1.6}) \cdot P_r/T_R \tag{7}$$

$$z_1 = (0.139 - 0.172/T_r^{4.2}) \cdot P_r/T_r \tag{8}$$

The acentric factor ω determines which substance is being simulated. Due a large amount of domestic compressors use isobutene as refrigerant, the selected acentric factor has been the corresponding to this fluid (0.18).

2.2 Turbulence modeling

The intrinsic turbulence associated to the chaotic fluid movement inside the muffler is modeled using TermoFluids (Lehmkuhl *et al.*, 2007), which has an extended library of turbulence models developed. The chosen one for this article is the Wall-Adapting Local Eddy-viscosity model (WALE) (Nicoud, F. and Ducros., 1999), which has been demonstrated to have a proper behavior near walls even with coarser grids compared with other models.

$$\mu_{SGS} = \rho \left(C_\omega V^{1/3} \right)^2 \frac{tr(S \cdot S^T)^{3/2}}{tr(\bar{S} \cdot \bar{S}^T)^{5/2} + tr(S \cdot S^T)^{5/4}} \tag{9}$$

$$S = \frac{1}{2}\left(G(\bar{u}')^2 + G^T(\bar{u}')^2\right) - \frac{1}{3} I\left(G(\bar{u}')^2\right) \tag{10}$$

$$\bar{S} = \frac{1}{2}\left(G(\bar{u}') + G^T(\bar{u}')\right) \tag{11}$$

Where the operator $G(\varphi)$ is the gradient matrix operator presented previously and I is the identity matrix.

2.3 Solver properties

Summarizing, the properties which the used solver has are:

- The convective and diffusive terms have been discretized using second order schemes. These schemes have been chosen to ensure the preservation of the kinetic energy (Jameson 2008, Baez et al. 2014, Pedro et al. 2015).
- At inlet and outlet, two buffer zones are used in order to assure stability during the simulation.
- Temporal evolution of the equations is computed via Runge-Kutta integration method, RK3. Time step is computed at step with a CFL 0.5. We remark the requirement that the used time step has to be able to compute not only the hydrodynamic behavior of the simulation but also the acoustic; hence, the maximum velocity of the simulation is the speed of sound (no supersonic Mach numbers are expected).
- LES turbulence model with WALE model which has produced overall good results without the additional effort to include new scalar equations to be resolved such as k-ε or k-ω models.
- Gas properties have been calculated at each time step using ideal gas equation with compressibility factor correction.

3. COMPUTATIONAL DOMAIN AND BOUNDARY CONDITIONS

3.1 Boundary conditions

The detailed simulation of the whole compressor with a three dimensional modeling is still not possible even with High Performance (HPC) facilities. Hence, the muffler has to be simulated as a part of the whole system but, at the same time, respecting the effect it produces to the whole compressor.

For this reason, first a 1D simulation of the whole compressor is performed in order to extract the values at both inlet and outlet of the muffler, in order to obtain the boundary conditions which couple the element with the whole system.

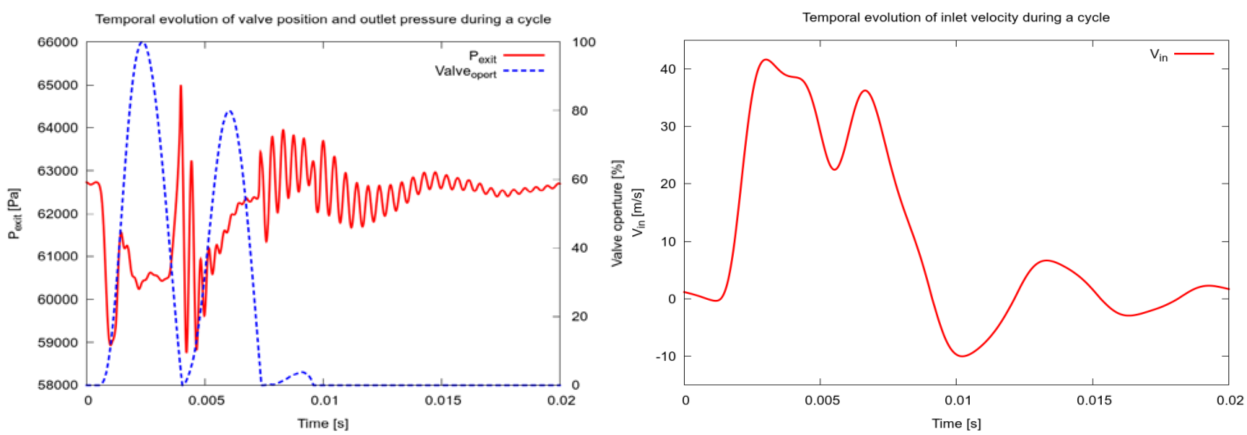

Figure 1: Boundary conditions at a) Outlet: Pressure and valve position and b) Inlet: velocity profile

Using the previous values as boundary conditions at both inlet and outlet, the simulation of the muffler becomes a reality. Hence, the velocity is imposed at the inlet of the element while a mixed boundary condition imposing valve position and pressure is set at the outlet. This mixed condition behaves as a non-slip wall boundary condition or as an outflow boundary condition by imposing the pressure depending of the valve's position. Summarizing, these both boundary conditions, at inlet and outlet, extracted from a one-dimensional simulation of the whole compressor, make feasible the simulation of a single element but taking into account, to some degree, its effect to the whole system. Finally, the condition applied at the inner walls of the muffler is an adiabatic non-slip boundary condition.

3.2 Computational domain

The domain selected to perform the simulation enlarges the muffler geometry as well as two buffer zones in order to attenuate spurious oscillations which can occur during simulation and ensure numerical stability during the computation.

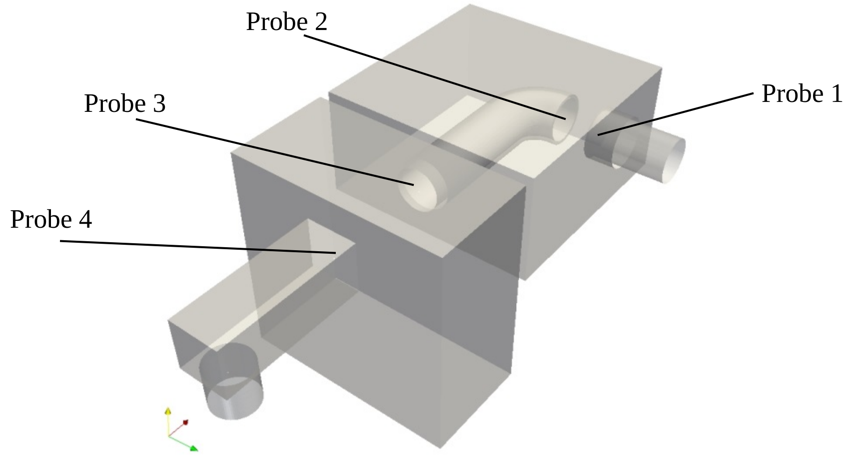

Figure 2: Computational domain and probes location

Inside the domain, where maximum precision is mandatory, schemes which preserve the kinetic energy, such as Symmetry Preserving schemes, are used in the discretization whereas up-winding techniques like upwind discretization schemes are used in buffer layers as has been previously commented. The use of a hybrid discretization is able to ensure numerical stability due to domain truncation at boundaries while in the inner domain the energy, and consequently noise and pressure perturbations, are not damped by the discretization.

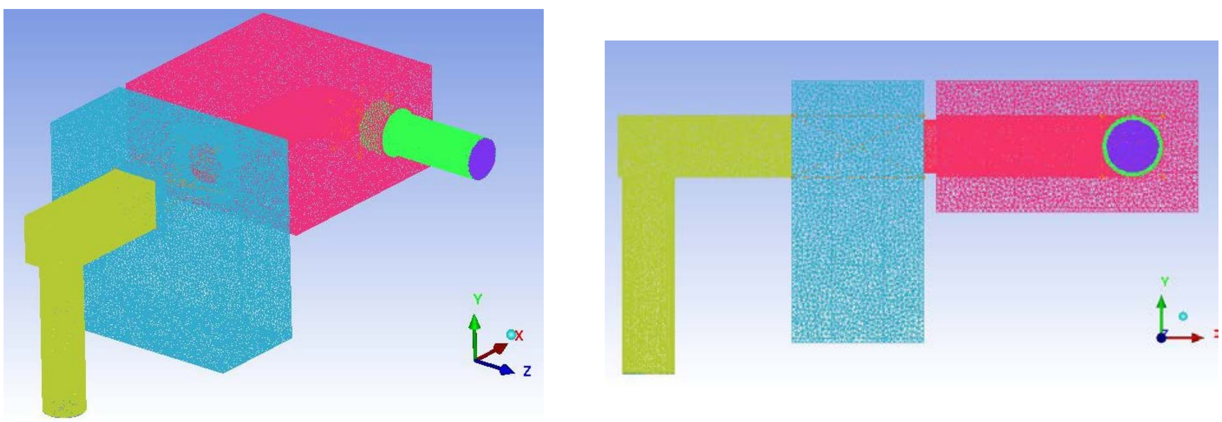

Figure 3: Isometric and front view of the used mesh

A tetrahedral unstructured mesh of approximately 2 Million Control Volumes is used. In order to correctly capture fluid expansion as well as pressure gradient at walls, the mesh is refined at the beginning and the end of all the tubes inside the muffler as well as at the walls of the computational domain. Furthermore, the quality of the inner cells has been set by iteration as a minimum aspect ratio value of 0.4 in order to improve the overall results of the simulation.

4. COMPUTATIONAL RESULTS

4.1 Hydrodynamic results

In this section, the results obtained from the transient three-dimensional numerical simulation of the studied muffler are commented. First, the velocity magnitude inside the muffler will be analyzed at several time localizations in order to check muffler's behavior qualitatively.

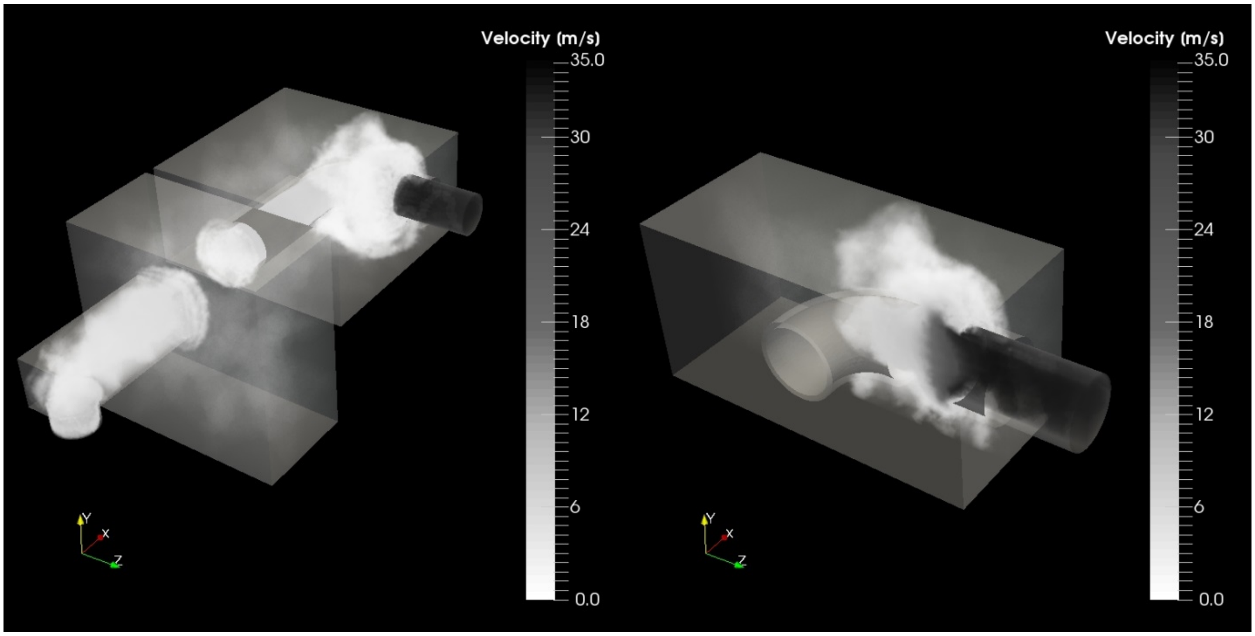

Figure 4: Velocity magnitude at valve maximum opening in a) the entire muffler and b) end of the inlet pipe.

The previous pictures show the velocity magnitude inside the muffler when the valve is fully open (0.0023 sec). At this point of the cycle the inlet flow has not reached the outlet, hence the outflow consists in the remnant fluid of the previous cycle. This could be observed in the expansion of the fluid at the end of the inlet pipe; if the fluid is still expanding this means it clearly hasn't reached the outlet. The maximum velocity during all the cycle is achieved during this period of time, when the outflow reaches approximately 40 m/s.

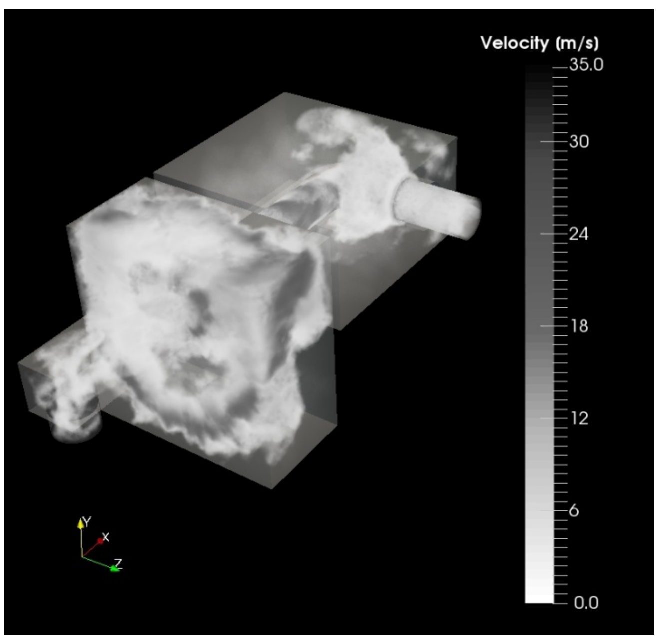

Figure 5: Velocity magnitude at valve closure in the entire muffler.

Figure 5 shows the velocity field when the valve is closed, at 0.0095 seconds. As can be seen, the velocity magnitude at the exit is practically 0, consisting in just small fluctuations. However, the rest of the domain has a clearly non null value. At the first expansion chamber could be observed how the fluid is still moving towards the muffler due to the form the expansion jet has. Thus, the chamber is accumulating mass when the valve has already

closed. Finally, is important to notice the velocity at the first chamber has only noticeable values at the near zone of the expansion tube, while the fluid at the rest of the chamber behaves as a fluid at rest state.
On the other hand, the second expansion chamber shows how the fluid is still moving and expanding. This happens as a conjunction of the previous facts: the valve has closed and consequently the fluid cannot go to the compression chamber but at the same time there is fluid coming from the inlet and first chamber.

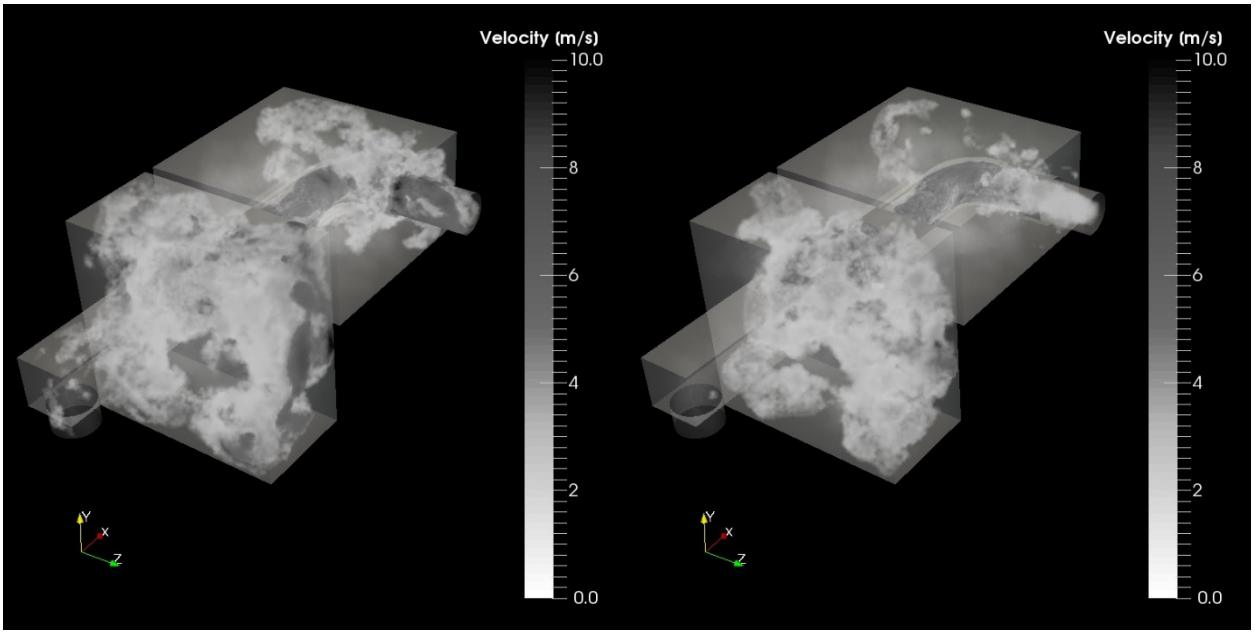

Figure 6: Instantaneous velocity field at a) 0.012 and b) 0.015 seconds

The previous pictures show the velocity field at 0.0125 and 0.015 seconds. These two instants have been selected because two facts could be observed: first, how the velocity magnitude starts to decrease (note the selected scale); second, how the maximum value is located at the inner pipe which communicates both chambers. This last fact comes from recirculation of fluid that lives between the first chamber and the second one during the part of the period outlet is closed; this back and forth movement is slowly decreased until the fluid stays at rest.

Apart from the instantaneous velocity fields, the pressure at several inner points of the muffler has been saved during the simulation, in order to study its temporal evolution which will be useful in a posterior acoustic analysis of the results. These points can be observed in figure 2.

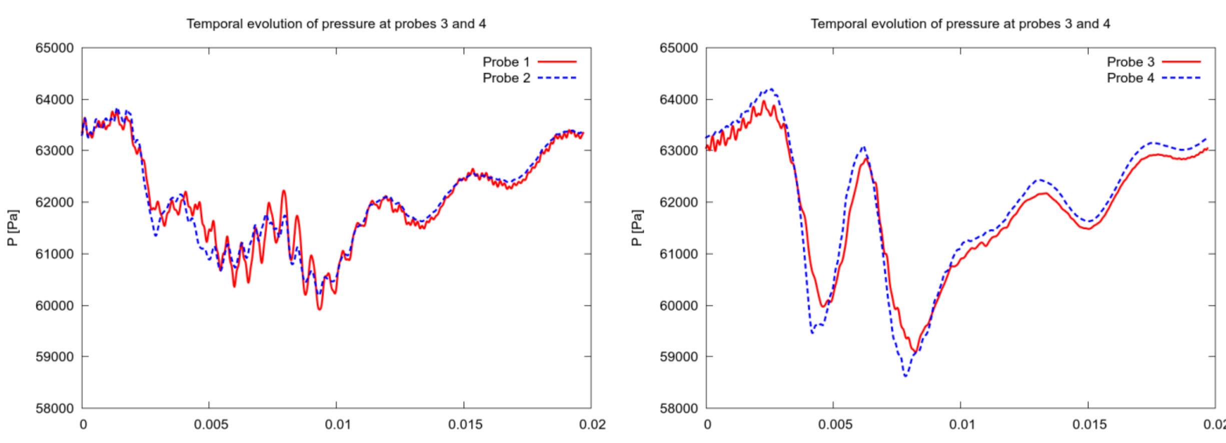

Figure 7: Temporal evolution of pressure at several locations

Both figures show a similar pattern: an initial pressure drop, with more or less superimposed oscillations until half cycle approximately, and a rise in pressure during the second half of the cycle until achieving initial values. The initial pressure drop is explained by the mass outgoing of the element; while the rise in pressure during the second half is explained by positive mass flow entering the muffler.

In figure 7, it can be observed how, apparently, probe 1 has larger oscillations than probe 2 even when the main purpose of the muffler is to attenuate the oscillations at the inlet. This happens due fluid behavior at the end of the inlet pipe is similar to a jet and consequently oscillations which hadn't been taken into account appear. This is checked during the second half of the cycle, when this jet-like behavior stops and these oscillations disappear.

The second set of probes doesn't show the commented oscillations, mainly because velocity magnitude at the second expansion is lower than in the first one. This set of probes show how the peaks of the oscillations are attenuated in the second chamber.

Furthermore, the pressure drop across the muffler during the cycle as well as the ratio between pressures at inlet and outlet can been computed. A pressure ratio similar to 1, or equivalently a pressure drop closer to 0, will indicate a good performance of the muffler from an hydrodynamic point of view due the presence of this element has as objective reduce pressure fluctuations without introducing additional losses, such as additional pressure drop, to the compressor.

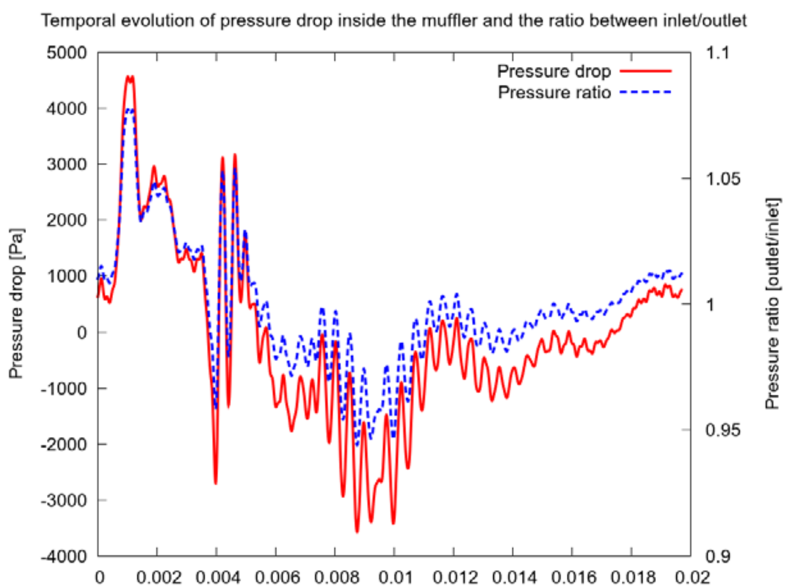

Figure 8: Pressure drop and ratio inside the muffler during a cycle

The previous figure shows how the pressure drop oscillates between 4500 and -3500 Pascals. Negative values are no surprise due as has been commented previously, fluid started to accumulate near the exit and hence the pressure is expected to grow more than in inlet when this happens. On the other hand, pressure ratios values oscillate near 1, which means the studied muffler doesn't affect the overall performance of the compressor.

4.2 Acoustic results

The acoustic behavior of the simulated muffler is studied via transforming the obtained pressure signals in the temporal domain to the spectral domain. This methodology permits studying which frequencies are being attenuated as well as if several resonances exist inside the muffler. By using a CFD simulation instead than simulating just the propagation of acoustic waves, two different acoustic waves exist:

- Waves which exist at the outlet of the muffler and are propagated through the inlet.
- Waves which are generated inside the muffler as a flow-induced noise.

Hence, the key point of this methodology is that is possible to take into account the noise generated by the muffler itself rather than just considering the muffler as an element which propagates noise but doesn't generate.

Figure 9 shows the spectrum of the pressure signals at both inlet and outlet of the muffler obtained after a Fourier Transform of the time dependent data. The ratio between the two signals is known as transmission losses (TL) of the muffler that shows how the element is capable to reduce pressure oscillations from the outlet (acoustic inlet) to the inlet (acoustic outlet); according to Lee (2002) the obtained parameter in this simulation would be more approximate to the insertion losses (IL) of the muffler instead of TL due the flow induced noise of the muffler is being taken into account. Regarding this measure, the obtained results in this simulation show good agreement with the ones of Lee (2002).

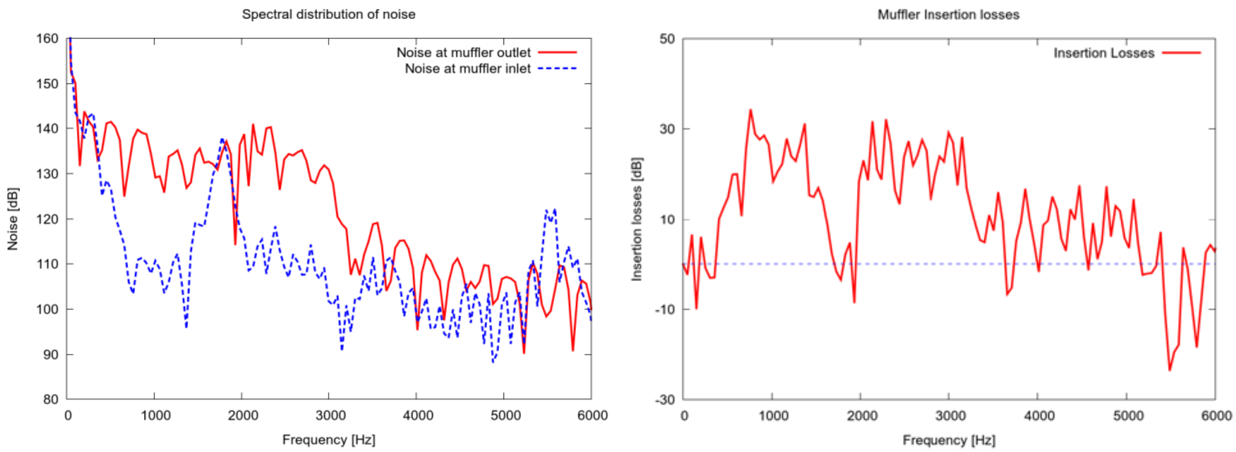

Figure 9: Noise at inlet and outlet and Insertion Losses of the muffler

Additionally, the spectrum at the different probes has also been computed to study how the different elements inside the muffler affect noise reduction. Moreover, the equivalent noise at each probe has been calculated to understand how it is reduced. The obtained results show good performance of the simulated muffler in the different studied positions, being the larger levels of noise those near the outlet of the muffler.

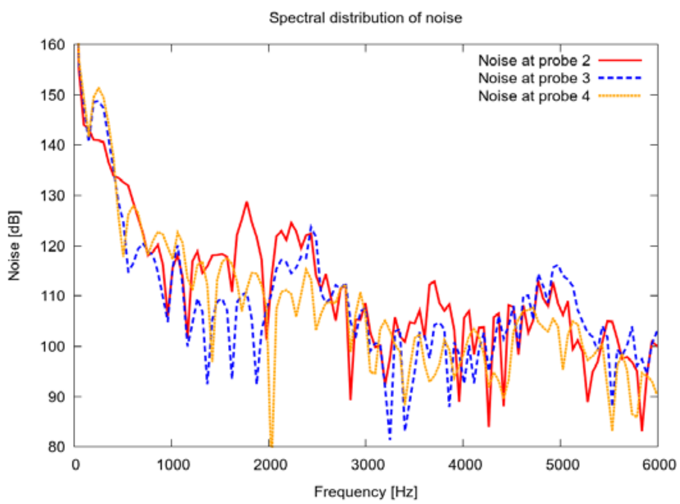

Figure 10: Noise at different locations inside the muffler

Table 1: Equivalent noise at different locations inside the muffler

Probe	1	2	3	4	Outlet
Noise [dBA]	153.086	153.24	155.588	156.845	157.367

5. CONCLUSIONS

The conclusions which can be extracted from the three-dimensional simulation of an academic muffler are:

- The present article uses a code able to predict numerically hydrodynamic and acoustic behavior in mufflers.
- The overall pressure inside the compressor drops after the valve opening. During the second half of the cycle the pressure rises achieving the values at the initial cycle time.
- During the second part of the cycle the total net mass flow entering the muffler is positive. However, several backflows occur.
- Jet-flow like behavior at the end of the inlet tube generates additional oscillation frequencies related to self-induced noise inside the muffler.
- The acoustic results show muffler is able to attenuate oscillations and good agreement with other authors.

NOMENCLATURE

Variables

ρ	Density	(kg/m^3)
u	Velocity vector	(m/s)
p	Pressure	(Pa)
T	Temperature	(K)
R	Ideal gas constant	(J/mol·K)
ω	Acentric factor	(-)
z	Compressibility factor	(-)
μ_{SGS}	Subgrid-scale viscosity	(Pa·s)
C_ω	WALE coefficient	(-)
$V^{1/3}$	Filter length	(m)

Subscript

r	Reduced value

Operators and matrices

Ω_c	Mass discrete operator
M	Divergence discrete operator
C	Convective discrete operator
D	Difusive discrete operator
G	Gradient discrete operator
τ	Shear stress tensor
I	Identity matrix

Superscript

$-$	Filtered value
$'$	Small scale component
T	Transposed matrix

REFERENCES

Baez, A., Pedro, J., Lehmkuhl, O., Trias, X., Perez Segarra, C.D. 2014. A filtered kinetic energy preserving methodology for large eddy simulations of compressible flows on unstructured meshes. . Kaliningrad.

Baez, A., Pedro, J., Lehmkuhl, O., Rodriguez, I., Perez Segarra, C.D. 2014. Comparing Kinetic energy preserving and Godunov schemes on the flow around a NACA0012. *11th European Conference on Computational Fluid Dynamics*. Barcelona.

Choi, J.M., Joo, J.M., Oh, S.K., Park, S.W, 2000, Smart suction muffler design for a reciprocating compressor. *International Compressor Engineering Conferece*. Purdue.

Done, V., Ventakesham, B., Tamma, B., Soni, K., Dey, S., Angadi, S., GP, V. 2014 Muffler Design for a Refrigerator Compressor. *International Compressor Engineering Conferece*. Purdue.

Jameson, A. 2008. Formulation of Kinetic Energy Preserving Conservative Schemes for Gas Dynamics and Direct Numerical Simulation of One Dimensional Viscous Compressible Flow in a Shock Tube Using Entropy and Kinetic Energy Preserving Schemes, *J. Sci. Comput*., v.34, pp.188-208.

Lee, J.H., An, K. H., Lee, I. S. 2002, Design Of The Suction Muffler Of A Reciprocating Compressor. *International Compressor Engineering Conferece*. Purdue.

Lehmkuhl, O., Perez-Segarra, C.D., Soria, M., Oliva, A. 2007, TermoFluids: A new Parallel unstructured CFD code for the simulation of turbulent industrial problems on low cost PC cluster. *Proceedings of the Parallel CFD 2007 Conference*, Springer, pp. 275–282.

Lopez, J. 2016, *Parallel object-oriented algorithms for simulation of multiphysics. Application to thermal systems.* Universitat Politècnica de Catalunya.

Lopez, J., Ruano, J., Lehmkuhl, O., Rigola, J., Oliva, A. 2015, Compressible 1D-3D simulation of a muffler with pseudosound prediction levels. *24th International Congress of Refrigeration*. Japan.

Pedro, J., Baez, A., Lehmkuhl, O., Perez, C., Oliva, A. 2015. On the extension of RANS/LES methods from incompressible to compressible transonic turbulent flows with SBLI. *8th International Symposium on Turbulence, Heat and Mass Transfer*. Sarajevo.

Poinsot, T.J. 1992, Boundary conditions for direct simulations of compressible viscous flows, *Journal of Computational Physics*. 101 (1): 104 – 129.

Rigola, J. 2002, *Numerical Simulation and Experimental Validation of Hermetic Reciprocating Compressors. Integration in Vapour Compression Refrigerating Systems*. CTTC, Terrassa, 112 p.

Roe, P.L. 1981, Approximate riemann solvers, parameter vectors and difference schemes, *Journal of Computational Physics*. 43 (2): 357 – 372

Sarioglu, K., Ozdemir, A.R., Orguz, M., Kaya, A., 2012, An experimental and numerical analysis of refrigerant flow inside suction muffler of hermetic reciprocating compressor. *International Compressor Engineering Conference*. Purdue.

Soedel, W. 1992, *Mechanics, simulation and design of compressor valves, gas passages and pulsation mufflers*. Purdue University, 262 p.

Trias, F.X., Lehmkuhl, O., 2011. A self-adaptive strategy for the time integration of Navier–Stokes equations. *Numerical Heat Transfer*, Part B 60, 116–134.

ACKNOWLEDGEMENTS

The authors acknowledge the collaboration between CTTC-UPC and Termo Fluids, S.L. company (C06550).
This work was supported by the Agència de Gestió d'Ajuts Universitaris i de Recerca (AGAUR), Catalonia, grant FI-DGR 2015.